Tug-of-war between dissimilar teams of microtubule motors regulates transport and fission of endosomes

Virupakshi Soppina, Arpan Kumar Rai, Avin Jayesh Ramaiya, Pradeep Barak, and Roop Mallik[1]

Department of Biological Sciences, Tata Institute of Fundamental Research, Homi Bhabha Road, Colaba, Mumbai 400005, India

Intracellular transport is interspersed with frequent reversals in direction due to the presence of opposing kinesin and dynein motors on organelles that are carried as cargo. The cause and the mechanism of reversals are unknown, but are a key to understanding how cargos are delivered in a regulated manner to specific cellular locations. Unlike established single-motor biophysical assays, this problem requires understanding of the cooperative behavior of multiple interacting motors. Here we present measurements inside live *Dictyostelium* cells, in a cell extract and with purified motors to quantify such an ensemble function of motors. We show through precise motion analysis that reversals during endosome motion are caused by a tug-of-war between kinesin and dynein. Further, we use a combination of optical trap-based force measurements and Monte Carlo simulations to make the surprising discovery that endosome transport uses many (approximately four to eight) weak and detachment-prone dyneins in a tug-of-war against a single strong and tenacious kinesin. We elucidate how this clever choice of dissimilar motors and motor teams achieves net transport together with endosome fission, both of which are important in controlling the balance of endocytic sorting. To the best of our knowledge, this is a unique demonstration that dynein and kinesin function differently at the molecular level inside cells and of how this difference is used in a specific cellular process, namely endosome biogenesis. Our work may provide a platform to understand intracellular transport of a variety of organelles in terms of measurable quantities.

asymmetric motor competition | coordination of motors | molecular motor dynein kinesin | regulation of bidirectional motion |

Motor proteins of the kinesin and dynein families (1) use energy from ATP hydrolysis to walk along microtubules (MTs). Most kinesins move to the MT-plus end (away from the nucleus) whereas dynein moves to MT-minus end (toward the nucleus) while carrying cargo such as lipid droplets, endosomes, mitochondria, vesicles, and virus. Multiple motors of both kinds usually reside on a single cargo, and their opposing activity leads to bidirectional motion of cargos with frequent reversals. This opposing motor activity appears to be regulated to bias motion in a net plus or minus direction and consequently deliver many cargos to desired spatiotemporal locations (2, 3). The cause and the mechanism of reversals during transport are unknown, but are of obvious importance in understanding how this transport may be regulated.

Two models are proposed to explain reversals: a coordinated switching of motor activity and a tug-of-war (TOW) between opposite motors (2, 3). In the widely accepted switching model, nonmotor regulatory proteins activate/inactivate motors in a mutually exclusive manner: As a result, opposite motors never generate force against each other. In contrast, TOW posits that opposite motors actually generate force against each other: One team of motors wins to detach the other and effect a reversal in its favor. It has not been possible to prove either model because the available experimental evidence (2–4) is indirect and difficult to interpret (5, 6). Because switching is dictated by external cues, the number of motors and/or single-motor properties is of secondary importance. In contrast, these numbers and proper-

ties are the very defining parameters of TOW-mediated bidirectional motion (5, 6). If indeed TOW can be demonstrated, determining these parameters for an ensemble of motors engaged in TOW is an exciting experimental challenge. Are motors adapted by single-molecule design to work together in this ensemble? If so, how does this adaptation help in regulating the TOW? This becomes especially relevant because fission of endosomes from opposing motor forces has been described earlier (7). The nature of this problem requires biophysical measurement of motor activity on single cellular cargoes because other methods cannot report on the active number of motors in real time. Unfortunately, experiments with kinesin- and dynein-coated plastic beads (8) are of limited use because the in vivo motor configuration cannot be reproduced on the surface of a bead.

Here we show that in sharp contrast to prevailing models of coordinated switching, kinesin and dynein on an endosome engage in TOW to effect reversals. This is done through experiments at three levels of complexity: inside live *Dictyostelium* cells, in a cell extract, and with beads coated with purified motors. We combine these assays with Monte Carlo simulations to elucidate how the cell uses certain dissimilarities between opposing motor teams to regulate the TOW. The regulation results in net minus-directed transport concurrent with TOW-mediated reversals that lead occasionally to fission of endosomes. Both of these processes are required to maintain a balance between the endosomal degradation and recycling pathways in mammalian cells (9–11). Finally, we support the general relevance of our findings by observing a similar mechanism of TOW-mediated endosome transport in HeLa cells.

Results

[Table S1](#) provides detailed statistics on all data reported in this paper.

Bidirectional Motion of Endosomes Is Mediated by Tug-of-War Between Microtubule Motors. We observed bidirectional motion of organelles in agar-flattened *Dictyostelium* cells (12), an established eukaryotic model system for intracellular transport and phagocytic/endocytic pathways (13). Most motile organelles were likely endosomes, as verified by a fluorescent endocytic marker (*Methods*). Individual endosomes could be video tracked with high precision (*Methods*). Trajectories revealed directed motion and likely reversals on a single MT, because endosomes retraced exactly the same path over a long distance after reversal (Fig. 1*A*). Motion close to reversals was projected along a straight line (presumed to be a MT) to obtain position versus

CELL BIOLOGY

Fig. 1. Tug-of-war between kinesin and dynein on endosomes inside *Dictyostelium* cells. (*A*) Trajectory of a reversal of an endosome inside a *Dictyostelium* cell in an *x–y* plane obtained from video tracking. Prereversal (grey circles) and postreversal motion (black circles) shows a close overlap over long distances, indicating that the reversal is along a single microtubule. (*Inset*) Part of an agar-flattened *Dictyostelium* cell is shown. The cell boundary is outlined (black dotted line). Two endosomes (circled) and their trajectories (white lines) are schematized. Note the reversals in direction. (Scale bar, 5 μm.) (*B*) Motion of another endosome close to a reversal is projected along a microtubule by assuming the microtubule to be a straight line. A slow tug-of-war (TOW) segment is sandwiched between fast motion. The direction of motion (plus or minus) is not determined (see main text). (*Upper Inset*) A time series of images (150 msec apart) of an endosome during reversal. The microtubule orientation is approximately vertical. Note the slowing down and elongation of the endosome, interpreted as a TOW between motors (also see Movie S1 and Movie S2). (*Lower Inset*) Elongation of this endosome is quantified manually using images from successive frames of Movie S1. Endosome length (distance between front and rear ends along direction of motion) is plotted as a function of time. There is a 33% increase in the length during TOW. TOW lasts for ≈1.3 sec.

time plot of the endosome along the MT (Fig. 1*B*). The slope of this plot at any time is the instantaneous endosome velocity. This procedure revealed a slow segment sandwiched between fast motion, making the reversals distinctly "triphasic." The velocity before and after reversal (≈2 μm/sec; Table S1) is in agreement with earlier reports (14, 15). Slow segments were often long (≈1 sec; Table S1), concomitant with visible endosome elongation along the direction of motion (*Insets*, Fig. 1*B*; Movie S1) and occasional fission (Movie S2). Because the endosome size and TOW duration are variable, we quantified the fractional increase in endosome length [= (maximum length during TOW–average length outside TOW)/average length outside TOW] for endosomes >500 nm in diameter. For example, this increase is 0.33 [= (1.6 − 1.2)/1.2] for the endosome in Fig. 1*B* (see *Lower Inset*). Averaged over all in vivo reversals, this value was 0.25 ± 0.10 (mean ± SD), showing an ≈25% increase in endosome length during TOW-mediated reversals.

The elongation, fission, and slower velocity demonstrate unambiguously that opposite motors apply force against each other to induce reversals, as in a molecular TOW. To the best of our knowledge, this is a unique experimental demonstration that reversals during bidirectional motion are mediated by TOW. We could clearly detect a TOW for 63% of reversals by scoring for slow "TOW segments" (defined as velocity <500 nm/sec for

Fig. 2. Motion of *Dictyostelium* endosomes on polarity-labeled microtubules. (*A*) In vitro reversals of endosomes along polarity-labeled microtubules. Video tracks of a plus → minus (*Left*) and minus → plus (*Right*) reversal are shown. Sharp changes in velocity occur at the beginning and end of the tug-of-war (TOW). The TOW segment has negative velocity for both reversals, indicating elongation toward the minus end with the plus end of the endosome static (see main text; also see Table S1). The microtubule orientation is schematized. The *Inset* shows a time series of images (150 msec apart) of the endosome undergoing minus → plus reversal. Note slowing down and elongation along the microtubule during TOW. Also note how the plus end of the endosome is static during TOW. (*B*) Motion in the optical trap of a plus-moving endosome likely driven by one kinesin. Note the long plateaus before motor detachment, where kinesin is "stalled." The stall force for this endosome is 5.6 pN, corresponding to a mean displacement of ≈180 nm from the center of the optical trap. (*C*) Motion in the optical trap for a minus-moving endosome likely driven by multiple dyneins. Note frequent detachments against load applied by the trap (compare with kinesin). This endosome walked out of the trap at an ≈4.5-sec time point

>150 msec; see Table S1). Intriguingly, TOW segments almost always showed a significant slope (i.e., a nonzero velocity; Fig. 1*B*). An equal elongation of the endosome toward both (plus and minus) directions should yield no net motion and therefore zero velocity during TOW. The slope implies an inherent asymmetry in the function of motor teams—one team is winning the TOW. We also observed endosome motion in HeLa cells (see *SI Text*). The close similarity of these reversals (triphasic nature and slope during TOW; compare Fig. S1*B* with Figs. 1*B* and 2*A*) makes it likely that a similar TOW mechanism operates in mammals. Apart from endosomes, shape changes during motion are reported for mitochondria (16).

To understand mechanistic details of this TOW, it is necessary to determine the composition of opposing motor teams, the identity of the winning/losing teams, and the single/cooperative motor function within these teams. The first requirement for such analysis is knowledge of MT polarity—only then can motor activity be ascribed to plus/minus motor(s). Unfortunately, the complicated MT structure of *Dictyostelium* (13) did not permit reliable identification of MT polarity in vivo.

In Vitro Reconstitution of Endosome Motion: Tug-of-War and Nature of Reversals. To circumvent the above problem, we reconstituted in vitro motion of organelles from a postnuclear supernatant (PNS) of *Dictyostelium* cells (*Methods*). The majority (>90%) of motile organelles in a crude extract from cells preincubated with rhodamine–dextran were fluorescent, identifying them as components of the endo-lysosomal pathway. It is known that endosome motion in *Dictyostelium* is driven by the dimeric DdUnc104 kinesin and cytoplasmic dynein (15, 17). We confirmed the presence and activity of both these motors on the endosome membrane (*SI Text*).

Motion was observed in vitro on single MTs that were polarity labeled at the minus end with nonfluorescent magnetic beads (18). This allowed us to resolve the plus/minus components of motion (and thereby the activity of kinesin/dynein) in video tracks of moving endosomes with high temporal and spatial resolution. Most motile endosome were refractile and spherical (≈500–1500 nm diameter; Movie S3) and moved rapidly over a long distance with frequent reversals in motion (Movies S4 and S5). In *Dictyostelium*, such organelles are identified as endosomal carriers between early and late endosomes (19). These have an internal membrane, which is likely to make them refractile. We first confirmed that there is no change in endosome motion between in vivo and vitro assays. This was done by assaying endosome motion in up to 200-fold diluted cell extract, whereupon no change in motion was observed (*SI Text*). We also performed optical trap-based measurement of the total force exerted by motors on endosomes directly inside cells and in cell extract. The fraction of endosomes escaping from the trap in both cases was the same, indicating that motor forces and by implication motor numbers are unchanged (*SI Text*).

We next focused on the mechanism of TOW-mediated reversals. The majority (82%; Table S1) of in vitro reversals were triphasic (Fig. 2*A*) and remarkably similar to in vivo reversals (compare Fig. 2*A* with Fig. 1*B*). Endosomes elongated at the reversal (*Inset*, Fig. 2*A*; Movies S4 and S5), demonstrating that opposite motors were pulling against each other. The fractional increase in endosome length during TOW (see earlier) was 0.32 ± 0.13. Interestingly, the plus-end extremity of endosomes was stationary during TOW, while the minus end continued moving. As a result, the center of mass of the endosome (and therefore its tracked position) shifted toward the MT minus end during TOW. This resulted in negative velocity during TOW for both plus → minus and minus → plus reversals (Fig. 2*A*; Table S1). From this result, we conclude that the average force in minus direction from dynein(s) exceeds the force of DdUnc104 kinesin(s) during TOW. DdUnc104 motor(s) are therefore under a "superstall" load (20) for the duration of the TOW (≈1 sec). During this time, DdUnc104 tenaciously anchors the plus end of the endosome to the MT, while the stronger team of dyneins pulls the minus end to elongate the endosome. The fraction of TOWs resulting in reversal could not be determined precisely because a slow velocity state (i.e., TOW) not succeeded by a reversal was often difficult to identify in the video tracks.

Fission of Tubular, Slow-Moving Endosomes. We also observed elongated tubules (length >2 μm) that are likely early endosomes (15, 19, 21). Tubules always moved slowly in a net minus direction (Movies S6 and S7; Table S1), with the rear (plus) end showing distinct steps, as if it was transiently "captured" onto the MT (Fig. S2). The front end continued to move smoothly in the minus direction with the rear captured—the tubule therefore exhibited stretching. Because of the extended MT contact of a tubule, multiple opposing motors likely engage in constant TOW. This leads to slow motion and frequent fission because neither team in the TOW will detach easily. A similar mechanism of TOW may operate in mammals because early endosomes from rat liver are tubular and exhibit reversals/fission while undergo-

ing net minus transport on MTs (7, 11). Because of their elongated shape, we did not attempt force measurements to determine motor numbers on tubules.

Mechanistic Details of Tug-of-War: Composition of Opposing Motor Teams. We used motion analysis and optical trap-based force measurements on endosomes to determine the number of opposing DdUnc104 and dynein motors, and the response of a class of motors to load applied by the other. Spherical endosomes were trapped and placed on polarity-labeled MTs. A subset of these endosomes with mean diameter of 657 ± 53 nm (*Methods*) was used to measure the response of motor(s) to load applied by the trap. As reported earlier (15), plus-directed endosome movements were less frequent and short, typical of motion driven by one to two motors (Table S1). At the laser power used, the maximum force exerted by the trap on endosomes is 6.3 ± 1.4 pN (see *Methods* for procedure of force estimation with endosomes). The majority (76%) of plus-moving endosomes stalled at 5.6 ± 2.2 pN in an optical trap (Fig. 2*B*). This value agrees with the stall force of a single purified DdUnc104 (see later experiments with motor-coated beads), indicating that the plus-directed endosome motion is usually driven by one DdUnc104 motor. The remaining 24% of endosomes escaped from the trap and are likely driven by two DdUnc104 kinesins because their run length was always <15 μm. Detachment of plus-moving endosomes under load was usually preceded by a long "stall" (velocity ≈0 at 5.5 pN; Fig. 2*B*). This shows that a single DdUnc104 can hold out tenaciously against ≈5.5 pN load for a rather long time.

Minus-directed endosome motion was fourfold more frequent than plus, in agreement with earlier reports (14, 15, 17). When assayed with an optical trap, 54% of minus-moving endosomes could not escape from the trap and exhibited forces between 4 and 6 pN. When released from the trap, these endosomes moved smoothly over a long distance (> 20 μm; Table S1; also see ref 18), typical of motion driven by four or more dyneins (22). These observations indicate that stall force of a single *Dictyostelium* dynein is significantly lower than ≈7 pN reported for yeast dynein coated onto beads (23). Note that our observation applies to endogenously assembled dynein on the surface of endosomes and may therefore be better representative of the in vivo situation. The remaining 46% of minus-moving endosomes escaped from the trap by exerting a force >6.3 ± 1.4 pN and again moved over a long distance (>20 μm). In contrast to plus, minus-moving endosomes showed repeated and rapid detachments/reattachments against load from the trap (Fig. 2*C*). The predetachment stall observed for plus motion was rarely seen for minus-moving endosomes (compare Fig. 2*B* and 2*C*).

The larger fraction of endosomes escaping in the minus direction (46%) compared to plus (24%) directly shows that the average motor force in the minus direction is larger. This validates our earlier explanation of negative slopes during TOW. Because 76% of plus-moving endosomes are driven by one DdUnc104, most instances of TOW would have one DdUnc104 opposing approximately five or more dyneins. Taken together, it appears that TOW-mediated endosome transport utilizes certain asymmetries: (*i*) The number of active DdUnc104s (one to two) is much smaller than that of dyneins (approximately four to eight), (*ii*) DdUnc104 kinesin is much stronger than dynein, and (*iii*) a single DdUnc104 remains attached tenaciously to the MT under load from many dyneins.

Kinesin- and Dynein-Coated Beads in an Optical Trap: Differences in Force and Response to Applied Load. To validate these asymmetries, we tested the motion of beads coated with DdUnc104 or dynein (purified from *Dictyostelium*; see *Methods* and Fig. S3) against controlled load in an optical trap. At the single-molecule limit (<30% MT binding, see ref. 8), dynein showed a run length of
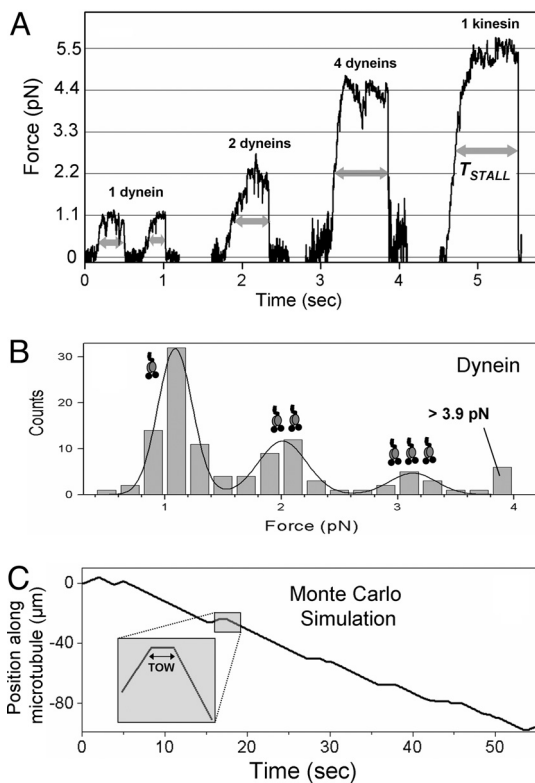
Fig. 3. Force and response to applied load of kinesin and dynein using motor-coated beads in an optical trap. (*A*) Stall in an optical trap for dyneins and DdUnc104 kinesin. T_{STALL} (thick double-headed arrows) is time spent above half-maximal load before detachment of motor(s). T_{STALL} increases with increasing dynein number and approaches the large value for a single tenacious kinesin (also see Table S1). (*B*) Histogram of stall force for dynein. The fit to the sum of three Gaussians (thick line) shows that the motor forces are additive. The obtained values of stall force for one, two, and three dyneins are 1.1 ± 0.3 pN, 2.0 ± 0.4 pN, and 3.1 ± 0.4 pN, respectively (Table S1). (*C*) Monte Carlo simulated trajectory of an endosome using experimentally determined input parameters. Four to eight weak dyneins are in a tug-of-war against one to two kinesins (see main text). Efficient minus transport with occasional reversals is seen. (*Inset*) Magnified view of a plus → minus reversal shows the zero-velocity TOW segment.

≈2 μm (Table S1), in agreement with data on dynein–dynactin complexes (24). A single dynein exerted a maximum force of 1.1 ± 0.3 pN (Fig. 3*A*). This agrees with in the vitro stall force of bovine dynein (22, 25, 26). A histogram of stall forces from measurements at varying dynein concentrations shows a periodicity of the single motor force (Fig. 3*B*) and therefore implies that motor forces are additive. This allows "counting" of active motor number on an endosome from a measurement of total force. To quantify the response of dynein to applied load we measured the time (T_{STALL}, see Fig. 3*A*) for which a motor-driven bead could sustain a load greater than half of its stall force (= $F_{STALL}/2$). The low value of T_{STALL} (= 0.22 ± 0.12 sec) for a single dynein shows that this motor detaches easily under an opposing load. The propensity to detach under load reduced gradually for multiple dyneins (compare T_{STALL} for one, two, and four dyneins in Fig. 3*A*; also see Table S1).

In similar experiments, single DdUnc104 showed a run length of 5.1 ± 2.5 μm and exerted a force of 5.5 ± 1.2 pN (Fig. 3*A*; Table S1; Fig. S4*B* for stall force histogram). This result agrees with earlier reports of run length (27) and force of dimeric Unc104 kinesin (28). This value of single-motor stall force from DdUnc104-coated beads is in excellent agreement with the stall force estimated for single DdUnc104 on plus-moving endosomes

(= 5.6 ± 2.2 pN, see earlier). This value supports the reliability of our stall force measurement for motors on the endosome. The same force is likely exerted by DdUnc104 in vivo (see earlier). DdUnc104 stalls usually exhibited a long plateau before motor detachment from the MT, similar to DdUnc104 on endosomes (Figs. 3*A* and 2*B*). The larger value of T_{STALL} (= 1.1 ± 0.55 sec; Table S1) shows that single DdUnc104 is much more tenacious against load than a single dynein.

The observed elongation of endosomes in the minus direction (Fig. 2*A*) shows that net minus force is larger than plus during TOW. Considering that the majority (76%) of plus endosomes stalled at ≈5.5 pN (and were therefore driven by one DdUnc104; see earlier), five or more dyneins (exerting ≥5.5 pN force, 1.1 pN each) would be pulling against one DdUnc104 during TOW. It appears that DdUnc104 can remain attached to the MT in this situation. To estimate this apparent tenacity of DdUnc104 against force >5.5 pN, we used a piezo stage to rapidly displace a DdUnc104-driven bead away from the optical trap center (Fig. S4*A*) and bring DdUnc104 under a superstall load of ≈7.7 pN (20). This would be the expected load from seven dyneins during TOW. In this state, DdUnc104 stayed attached to the MT for 0.7 ± 0.3 sec (Table S1), which is close to the duration of TOWs (≈1 sec). This tenacity permits DdUnc104 to hold out in a TOW against many dyneins—at this time, an endosome elongates toward the minus direction and may undergo fission. Forces of 11−18 pN are sufficient to form tubes from the endoplasmic reticulum and the Golgi membrane (29). Such forces can be achieved with one to two DdUnc104s in a TOW against five to eight dyneins.

Monte Carlo Simulations: The Need for Kinesin and Dynein to Be Different.

We did a Monte Carlo simulation of TOW-induced bidirectional motion to analyze the function of opposing motor teams. Using parameters obtained directly from our experiments (e.g., motor forces, T_{STALL}, attachment/detachment probabilities, etc.; see *SI Text*), observed characteristics of motion such as efficient minus transport, TOW-mediated reversals, and short plus runs could be reproduced (Fig. 3*C*; Table S1). Making dynein identical to kinesin in these simulations (stall force = 5.5 pN, T_{STALL} = 1.1 sec for both motors), but retaining the motor number asymmetry (to ensure net minus motion) abolished the TOW segment because the force imbalance detached one to two kinesins as soon as they engage against four to eight "strong" dyneins. *In silico* analysis of TOW-mediated bidirectional motion by others (6) also showed that using one to two kinesins against four to seven weak dyneins (stall force 1.1 pN) results in conversions between plus, TOW, and minus motions. The TOW state is abolished if multiple "strong" dyneins are used against one to two kinesins. This result is exactly what we observe in our experiments with endosomes.

Discussion

Asymmetric Motor Competition Model for Endosome Transport. We have directly demonstrated that reversals during endosome motion arise from a tug-of-war between oppositely directed microtubule motors. The resultant bidirectional motion and fission require three inequalities: (*i*) more dynein, less kinesin; (*ii*) weak dynein, strong kinesin; and (*iii*) detachment-prone dynein, tenacious kinesin. We formalize the requirement for these asymmetries and the transport arising out of it as an "asymmetric motor competition model" (AMCM) (see Fig. 4).

Why are these asymmetries needed? Dynein-mediated transport is important for endosomal sorting in mammalian cells (10) and *Dictyostelium* (13, 21, 30, 31). AMCM allows efficient minus transport driven by multiple dyneins, so that the moving endosome may encounter and fuse with later components of the endosomal pathway. Concurrent recycling of membrane requires TOW-mediated fission. To be effective, this TOW needs closely

Fig. 4. Asymmetric motor competition model (AMCM). A sequence of events for tug-of-war-mediated plus → minus and minus → plus reversals is schematized. A single kinesin is shown in a tug-of-war against six dyneins. Note endosome stretching in the minus direction in both cases, with the kinesin-attached plus end being almost stationary. One dynein exerts ≈1.1 pN force, whereas kinesin exerts ≈5.5 pN. Dynein is also more prone to detachment than kinesin under applied backward force (load). These asymmetries in number and single-motor properties combine to ensure net minus transport of endosomes with occasional reversals and fission (see main text).

matched opponents. However, using a large number of kinesins would bias the motion toward plus and therefore interfere with endosome degradation. The solution is to have sparse, but strong kinesins that can tenaciously anchor one end of the endosome to a MT upon attachment. This single kinesin almost matches the combined strength and tenacity of multiple (approximately six or more) dyneins to maintain a TOW over a period long enough to induce fission. Because the large number of dyneins ensures frequent minus-end motion, any occasional kinesin attachment immediately becomes a TOW. Our Monte Carlo simulations showed that no combination of single-motor properties and/or motor numbers other than AMCM can optimally achieve simultaneous exploration of space (for fusion with other endosomes) and fission (for recycling).

Possible Models for Sorting of Kinesin and Dynein on the Endosome Membrane During Tug-of-War. Randomly located kinesins and dyneins must sort away toward plus and minus halves of the endosome to make a TOW effective. Two models for this sorting come to mind: First, one kinesin located just by chance at the plus extremity of a minus-moving endosome binds stochastically to a MT (see Fig. 4). This kinesin opposes the bulk of minus-moving dyneins, thereby elongating the endosome. A second possibility is sorting during a TOW. Because the endosome membrane is deformable, membrane-bound kinesin(s) could walk past oppositely moving dyneins on adjacent protofilaments of a MT. This could sort motors so that the kinesin(s) ends up on the "plus half" and most dyneins on the "minus half" of the endosome, after which an effective TOW can happen. Note how using a

single kinesin is advantageous: Multiple kinesins and dyneins trying to walk past each other could jam up all of the protofilaments. Clustering of motors on lipid domains (27) within the endosome membrane may aid such sorting. The precise mechanism of motor sorting remains speculative at this time.

Minus and Plus Motors: Built Differently to Work Together? Dynein and kinesin are fundamentally different in single-molecule design and, by implication, in single-molecule function (1, 32). Dynein is likely a weaker motor because of its long force-generating arm. This feature may in turn be a steric adaptation (33) for multiple dyneins to function together, as seen here. Dynein may also function as a gear to take larger steps under low load (25, 34). Thus, there is little additional energy cost of using multiple dyneins against one kinesin when motors are not in a TOW. Dynein frequently transitions into a weakly bound state on the MT, where it is prone to detachment under load (Figs. 2*C* and 3*A*; also see ref. 22). Using multiple dyneins reduces the detachment rate under load and can therefore tune the outcome of a TOW against kinesin. In contrast to dynein, the tenacity of DdUnc104 kinesin is reminiscent of kinesin-1. For kinesin-1, the enzymatic cycle ensures that one strongly bound head is anchored to the MT when the other head searches for a binding site (20). These differences between plus- and minus-directed motors may be a general feature of bidirectional transport. Endosome fission in rat liver uses kinesin-1 and minus-directed kinesin-14 (7). Single kinesin-14 from *Drosophila* (also called *ncd*) detaches frequently from the MT, but multiple *ncd*s become processive and can move against sustained load in an optical trap (35). Therefore, we again have a situation similar to *Dictyostelium* endosomes, with DdUnc104 replaced by kinesin-1 and dynein replaced by kinesin-14. The general applicability of these findings for *Dictyostelium* is supported by our observation of a TOW during endosome reversals in HeLa cells (see *SI Text*, Fig. S1, and Movie S8).

To conclude, we have demonstrated that regulated bidirectional motion and fission of endosomes require a tug-of-war between different numbers of opposing motors with distinct single-motor properties. In vitro assays with motor-coated beads have measured single-molecule function of kinesin and dynein (1, 8, 20, 23, 25) and differences therein with increasing precision (36). However, the in vivo significance of these results has not been obvious. By extending such measurements to a real cellular cargo, we have shown why these differences are required and how they are used in a specific cellular process. Our demonstration of a TOW differs from prevailing models of coordinated motor function on lipid droplets, pigment granules, and other organelles (2). Because of its stochastic nature, TOW-mediated bidirectional transport is amenable to computer modeling, where novel regimes of transport can be explored. We have experimentally measured parameters relevant to the TOW and therefore opened the possibility for theory and experiment to go together in investigating the rich variety of intracellular transport.

Methods

Chemicals and Antibodies. All chemicals and antibodies were purchased from Sigma unless otherwise mentioned. An affinity-purified rabbit polyclonal antibody (gift from M. Koonce, Albany, NY) against the 78-kDa domain containing P-loops 1 and 2 was used to immunodetect dynein heavy chain (DHC).

Organelle Motion Inside *Dictyostelium* Cells. Cells were flattened onto coverslips by agar overlay (12). Motion was observed under differential interference contrast (DIC) illumination (100×, 1.3 NA Nikon objective) on an inverted microscope (Nikon TE-2000). Cells preincubated with rhodamine–dextran (2 mg/mL, 20 min) were observed in the fluorescence channel to identify endosomes (15).

Preparation and Motility of *Dictyostelium* Endosomes on Polarity-Labeled Microtubules. Preparation of a crude extract containing motile endosomes was essentially the same as reported elsewhere (15, 18). Motility was assayed at 22 °C in a flow cell (8) with 0.5 μL PNS added to a motility mixture [18.5 μL of LB/15% sucrose and 1 μL of a 20× ATP regenerating mix (= 20 mM ATP, 20 mM MgCl₂, 40 mM creatine phosphate, and 40 units/mL creatine kinase)]. MTs were polarity labeled using magnetic avidin-coated beads (18). Briefly, short biotinylated MT seeds were preferentially extended from the plus end with a mixture of normal (nonbiotin) tubulin and N-ethylmaleimide (NEM) tubulin and adhered to a polylysine-coated coverslip. Avidin-coated magnetic beads were magnetically sedimented onto MTs. The magnet was removed and unbound magnetic beads were washed out.

Purification of Kinesin and Dynein from *Dictyostelium*. Kinesin and dynein were purified from a high-speed supernatant (15, 17) by a microtubule affinity-based separation. Motors were released with ATP, and the releasate was centrifuged on a linear sucrose gradient to separate kinesin and dynein. Further details can be found in *SI Text*.

Video Tracking and Velocity Analysis. Frames were acquired with a Cohu 4910 camera (30 fps; no binning), digitized, and saved as audio video interleave (AVI) files. Each pixel measured 98 × 98 nm. Motion of single endosomes was tracked offline (37) with subpixel resolution (≈5 nm) by calculating the centroid of a cross-correlation image and analyzed as described (18, 22, 25).

Optical Trapping. Force measurement with motor-coated beads has been described elsewhere (8, 22, 25). In assays with cell extract, endosomes within a certain size range were visually selected for force measurement. The power spectrum (8, 22) of thermal fluctuation of trapped endosomes in motility buffer was measured using a quadrant detector and fitted to a Lorentzian to obtain a mean corner frequency (= 607 ± 130 Hz; see Fig. S5). A mean diameter (= 657 ± 53 nm) was measured from the peak-to-trough distance in a DIC image (38) of endosomes that were used to estimate force. Silica beads of known size served as a reference. The trap stiffness for endosomes (= 0.035 ± 0.008 pN/nm) was obtained from the aforesaid size and corner frequency after propagating the errors. The optical trap functioned as a Hookean spring out to ≈180 nm from the trap center for endosomes and beads (8). The close agreement between stall force for DdUnc104 on endosomes and beads supports the reliability of this method (Table S1). The method for force estimation inside cells is described in *SI Text*.

1. Vale RD (2003) The molecular motor toolbox for intracellular transport. *Cell* 112:467–480.
2. Welte MA (2004) Bidirectional transport along microtubules. *Curr Biol* 14:R525–R537.
3. Gross SP (2004) Hither and yon: A review of bi-directional microtubule-based transport. *Phys Biol* 1:R1–R11.
4. Gross SP, Welte MA, Block SM, Wieschaus EF (2002) Coordination of opposite-polarity microtubule motors. *J Cell Biol* 156(4):715–724.
5. Muller MJ, Klumpp S, Lipowsky R (2008a) Tug-of-war as a cooperative mechanism for bidirectional cargo transport by molecular motors. *Proc Natl Acad Sci USA* 105:4609–4614.
6. Muller MJ, Klumpp S, Lipowsky R (2008b) Motility states of molecular motors engaged in a stochastic tug-of-war. *J Stat Phys* 133:1059–1081.
7. Murray JW, Wolkoff AW (2003) Roles of the cytoskeleton and motor proteins in endocytic sorting. *Adv Drug Deliv Rev* 55(11):1385–1403.
8. Rice SE, Purcell TJ, Spudich JA (2003) Building and using optical traps to study properties of molecular motors. *Methods Enzymol* 361:112–133.
9. Soldati T, Schliwa M (2006) Powering membrane traffic in endocytosis and recycling. *Nat Rev Mol Cell Biol* 7(12):897–908.
10. Driskell OJ, Mironov A, Allan VJ, Woodman PG (2007) Dynein is required for receptor sorting and the morphogenesis of early endosomes. *Nat Cell Biol* 9(1):113–120.
11. Murray JW, Bananis E, Wolkoff AW (2000) Reconstitution of ATP-dependent movement of endocytic vesicles along microtubules in vitro: An oscillatory bidirectional process. *Mol Biol Cell* 11(2):419–433.
12. Fukui Y, Yumura S, Yumura TK (1987) Agar-overlay immunofluorescence: High-resolution studies of cytoskeletal components and their changes during chemotaxis. *Methods Cell Biol* 28:347–356.
13. Koonce MP (2000) Dictyostelium, a model organism for microtubule-based transport. *Protist* 151(1):17–25.
14. Ma S, Chisholm RL (2002) Cytoplasmic dynein-associated structures move bidirectionally in vivo. *J Cell Sci* 115:1453–1460.
15. Pollock N, Koonce MP, de Hostos EL, Vale RD (1998) In vitro microtubule-based organelle transport in wild-type Dictyostelium and cells overexpressing a truncated dynein heavy chain. *Cell Motil Cytoskeleton* 40:304–314.
16. Gennerich A, Schild D (2006) Finite-particle tracking reveals submicroscopic-size changes of mitochondria during transport in mitral cell dendrites. *Phys Biol* 3(1):45–53.
17. Pollock N, de Hostos EL, Turck CW, Vale RD (1999) Reconstitution of membrane transport powered by a novel dimeric kinesin motor of the Unc104/KIF1A family purified from Dictyostelium. *J Cell Biol* 147:493–506.
18. Soppina V, Rai A, Mallik R (2009) Simple non-fluorescent polarity labeling of microtubules for molecular motor assays. *Biotechniques* 46:297–303.
19. Neuhaus EM, Almers W, Soldati T (2002) Morphology and dynamics of the endocytic pathway in Dictyostelium discoideum. *Mol Biol Cell* 13(4):1390–1407.
20. Coppin CM, Pierce DW, Hsu L, Vale RD (1997) The load dependence of kinesin's mechanical cycle. *Proc Natl Acad Sci USA* 94(16):8539–8544.
21. Clarke M, Kohler J, Heuser J, Gerisch G (2002) Endosome fusion and microtubule-based dynamics in the early endocytic pathway of Dictyostelium. *Traffic* 3(11):791–800.
22. Mallik R, Petrov D, Lex SA, King SJ, Gross SP (2005) Building complexity: An in vitro study of cytoplasmic dynein with in vivo implications. *Curr Biol* 15:2075–2085.
23. Gennerich A, Carter AP, Reck-Peterson SL, Vale RD (2007) Force-induced bidirectional stepping of cytoplasmic dynein. *Cell* 131(5):952–965.
24. King SJ, Schroer TA (2000) Dynactin increases the processivity of the cytoplasmic dynein motor. *Nat Cell Biol* 2(1):20–24.
25. Mallik R, Carter BC, Lex SA, King SJ, Gross SP (2004) Cytoplasmic dynein functions as a gear in response to load. *Nature* 427:649–652.
26. Vershinin M, Xu J, Razafsky DS, King SJ, Gross SP (2008) Tuning microtubule-based transport through filamentous MAPs: The problem of dynein. *Traffic* 9(6):882–892.
27. Klopfenstein DR, Tomishige M, Stuurman N, Vale RD (2002) Role of phosphatidylinositol(4,5)bisphosphate organization in membrane transport by the Unc104 kinesin motor. *Cell* 109(3):347–358.
28. Tomishige M, Klopfenstein DR, Vale RD (2002) Conversion of Unc104/KIF1A kinesin into a processive motor. *Science* 297(5590):2263–2267.
29. Upadhyaya A, Sheetz MP (2004) Tension in tubulovesicular networks of Golgi and endoplasmic reticulum membranes. *Biophys J* 86(5):2923–2928.
30. Ma S, Chisholm RL (2001) Molecular motors and membrane traffic in Dictyostelium. *Biochim Biophys Acta* 1525(3):234–244.
31. Klopfenstein DR, Holleran EA, Vale RD (2002) Kinesin motors and microtubule-based organelle transport in Dictyostelium discoideum. *J Muscle Res Cell Motil* 23(7–8):631–638.
32. Mallik R, Gross SP (2004) Molecular motors: Strategies to get along. *Curr Biol* 14(22):R971–R982.
33. Vallee RB, Gee MA (1998) Make room for dynein. *Trends Cell Biol* 8(12):490–494.
34. Nan X, Sims PA, Xie XS (2008) Organelle tracking in a living cell with microsecond time resolution and nanometer spatial precision. *Chemphyschem* 9(5):707–712.
35. Higuchi H, Endow SA (2002) Directionality and processivity of molecular motors. *Curr Opin Cell Biol* 14(1):50–57.
36. Mallik R, Gross SP (2004) Molecular motors: Strategies to get along. *Curr Biol* 14:R971–R982.
37. Carter BC, Shubeita GT, Gross SP (2005) Tracking single particles: A user-friendly quantitative evaluation. *Phys Biol* 2:60–72.
38. Shtridelman A, et al. (2009) In vivo multimotor force–velocity curves by tracking and sizing sub-diffraction limited vesicles. *Cell Mol Bioeng* 2(2):190–199.